

Determining equilibrium osmolarity in Poly(ethylene glycol) / Chondrotin sulfate gels mimicking articular cartilage

S. Sircar^{a,e}, E. Aisenbrey^b, S. J. Bryant^{b,c,d} & D. M. Bortz^{a,c}

^a Department of Applied Mathematics, University of Colorado, Boulder, CO 80309

^b Department of Chemical & Biological Engg., University of Colorado, Boulder, CO 80309

^c BioFrontiers Institute, University of Colorado, Boulder, CO 80309

^d Material Science and Engineering Program, University of Colorado, Boulder, CO 80309

^e Corresponding Author (email: sarthok.sircar@colorado.edu)

August 29, 2020

Abstract

We present an experimentally guided, multi-phase, multi-species polyelectrolyte gel model to make quantitative predictions on the electro-chemical properties of articular cartilage. The mixture theory consists of two different types of polymers: Poly(ethylene glycol) (PEG), Chondrotin sulfate (ChS), water (acting as solvent) and several different ions: H^+ , Na^+ , Cl^- . The polymer chains have covalent cross-links modeled using Doi rubber elasticity theory. Numerical studies on polymer volume fraction and net osmolarity (difference in the solute concentration across the gel) show the interplay between ionic bath concentrations, pH, polymer mass in the solvent and the average charge per monomer; governing the equilibrium swelled / de-swelled state of the gel. We conclude that swelling is aided due to a higher average charge per monomer (or a higher percentage of charged ChS component of the polymer), low solute concentration in the bath, a high pH or a low cross-link fraction. However, the swelling-deswelling transitions could be continuous or discontinuous depending upon the relative influence of the various competing forces.

Keywords: Donnan pressure, polyelectrolyte gel, multi-phase mixture, hydrogel

1 Introduction

Articular cartilage is a polyelectrolyte biogel that forms a thin tissue layer lining the articulating ends of all diarthrodial joints in the body and contribute to the lubrication mechanisms in the joint [1]. The water phase of cartilage constitutes on average from 60-80 % of the total weight for normal tissue while the dominant structural components of the solid matrix are the collagen molecules and proteoglycans (PGs) [2]. The collagen fibrils are densely packed polymer strands with a high resistance against fluid flow [3], which helps in retaining the shape of the cartilage when compressed [4]. PG are macromolecules consisting of a protein

core to which are attached short chains of negatively charged glycosaminoglycans (GAGs) [5]. The primary GAGs associated with PGs in cartilage are chondroitin 4-sulfate, chondroitin 6-sulfate and keratan sulfate [4].

An increase in cartilage tissue hydration, governed by the density and the nature of fixed charges on the PGs as well as the density of the mobile counter ions in the interstitial fluid are the earliest signs of articular cartilage degeneration during osteoarthritis [3, 4]. For this reason the development of methods to quantify cartilage swelling have been of great interest for many years. Each PG-associated negative charge, on the polymer chain, requires a mobile counter-ion (e.g., Na^+) dissolved within the interstitial fluid in the gel to maintain electro-neutrality within the gel [6]. This gives rise to an imbalance of mobile ions across the gel interface. The excess of mobile ions colligatively yields a swelling pressure, known as the osmotic pressure [7], while the swelling pressure that is associated with the fixed charges on the polymer chain is known as the Donnan pressure [8]. The swelling pressure in articular cartilage is balanced by tensile forces generated in the collagen network [9]. Thus, changes in this internal swelling pressure, arising from altered ion concentrations of the external bath, or changes in the fixed charges on the polymer network will result in changes in tissue dimensions and hydration.

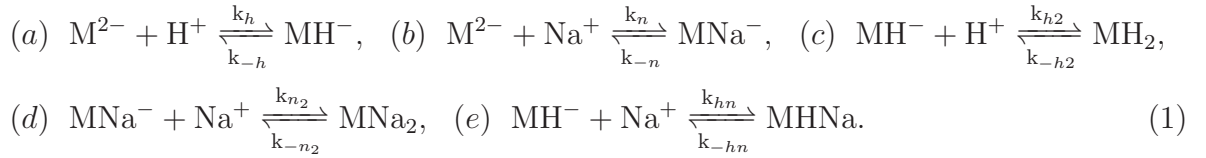
Previous work on polyelectrolyte gels builds on the classic work of Tanaka on hydrogels [10], and includes effects of osmotic pressure arising from the charge-induced Donnan equilibrium [11, 12], the Poisson-Boltzmann equation and Biot's theory of poroelasticity [13], as well as phenomenological modifications of Flory-Higgins theory to capture some effects of multi-ionic cations [14, 16]. Furthermore, in previous gel swelling literature, the Flory interaction parameter was either chosen to be a function of temperature alone or of temperature and polymer volume fraction [12, 15].

The purpose of this paper is to present a comprehensive model of polyelectrolyte gel swelling/deswelling mechanism, mediated by the dissolved ions in the solvent as well as covalent cross-links within the polymer chain. To calibrate the outcome of this model, in vitro set-up of cross-linked copolymerized poly(ethylene glycol) (PEG) chondroitin sulfate (ChS) and polymethacrylate gels were developed. The kinetic chains associated with polymethacrylate group represents less than one percent of the total hydrogel volume and therefore they are not considered in the model. PEG was chosen since it can be functionalized to enable cross-linking to form a 3-D matrix, a system that promotes the deposition of proteoglycans and collagen molecules when cartilage cells are encapsulated and emulates the mechanical strength, load bearing capabilities and resilience of cartilage tissue [17]. The ChS component serves two purposes: to mimic the biochemical environment of cartilage (since it is the main component of proteoglycans) and to introduce fixed negative charges into the network [18].

In the next section, we present the details of this model, including the equation of motion and interface conditions (§2.1), chemical potentials (§2.2) and the chemistry of the binding reaction at quasi-equilibrium conditions (§2.3). In §3, we provide the details of the gel swelling experimental set-up, while the results pertaining to the equilibrium configuration of these ionic gels under different electro-chemical stimuli are presented in §4. We conclude with a brief discussion of the implication of these results and the focus of our future directions.

2 Multi-species, multi-phase cartilage-gel model

We view the PEG-gel with negatively charged ChS strands in ionic solution, as a multi-component material, including solvent particles, polymers, and several ionic species. The polymer is assumed to be made up of two types of monomers which are either uncharged (i.e PEG segment of the polymer) or the charged units (which is the ChS segment of the polymer), denoted as M, and each of which carries a double negative charge (or M^{2-}). The positively charged ions in the solvent are Hydrogen (H^+) and Sodium (Na^+). The negatively charged ions could include Hydronium (OH^-) and Chloride (Cl^-). Because the negatively charged ions are assumed to be not involved in any binding reactions with the gel, acting only as counterions to positive charges, we identify these ions by the name Chloride. The binding reactions of the positively charged ions with the monomers are:



We assume that all the binding sites/charge sites are identical and the binding affinities for the different ions are different. The species M^{2-} , MH^- , MNa^- , MH_2 , MNa_2 and $MHNa$ are different monomer species, all of which move with the polymer velocity. The ion species are freely diffusible, but because they are ions, their movement is restricted by the requirement to maintain electroneutrality. Finally, because a small amount of water dissociates into hydrogen and hydronium, we are guaranteed that there are always some positive and negative ions in the solvent.

2.1 Equations of motion and interface conditions

Suppose we have some volume V of a mixture comprised of k types of particles each with particle density (number of particles per unit volume) n_j , and particle volumes ν_j , $j = 1, \dots, k$. From now on we will denote the quantities with subscript ‘‘1’’ related to PEG monomer species, subscript ‘‘2’’ related to ChS monomer species and subscript ‘‘3’’ related to solvent molecule. For each of these components there is a velocity, \mathbf{v}_j , the polymer network velocity $\mathbf{v}_1 = \mathbf{v}_2 = \mathbf{v}_p$ (the subscript ‘‘p’’ denotes polymer), the solvent velocity $\mathbf{v}_3 = \mathbf{v}_s$ and molecular species velocities \mathbf{v}_j , $j = 4, \dots, k$. The volume fraction for each of the polymer species (θ_1, θ_2) and the solvent ($\theta_3 = \theta_s$) are $\theta_i = \nu_i n_i$, $i = 1, 2, 3$; respectively. The particle conservation of polymer species implies that

$$\frac{\partial \theta_i}{\partial t} + \nabla \cdot (\mathbf{v}_p \theta_i) = 0, \quad i = 1, 2 \tag{2}$$

Suppose the ChS monomers constitute a fraction ‘ α ’ of the total number of monomers, n_m , (i.e., $n_2 = \alpha n_m$, $n_1 = (1 - \alpha)n_m$) and the volume ratio of the ChS to PEG monomers is β (i.e., $\nu_2 = \beta \nu_1$). Assuming that the other molecular species do not contribute significantly to the volume (i.e., we take $\nu_j = 0$, $j = 4, \dots, k$), conservation of total volume implies $\theta_1 + \theta_2 + \theta_3 = 1$. From Eq. (2), it follows that

$$\nabla \cdot (\theta_s \mathbf{v}_s + (\theta_1 + \theta_2) \mathbf{v}_p) = \nabla \cdot \left(\mathbf{v}_s + \theta_1 \left\{ \frac{1 + (\beta - 1)\alpha}{1 - \alpha} \right\} (\mathbf{v}_p - \mathbf{v}_s) \right) = 0. \tag{3}$$

Further, in subsequent calculations we make an assumption that the density of ions particles is insignificantly small compared to the particle density of polymer and solvent, i.e. $\sum_{j \geq 4} n_j \ll n_s + n_m$. The motion of the polymer and solvent phase of this multi-component mixture is governed by the Stokes equation for Newtonian fluid, which are

$$\nabla \cdot (\theta_p \sigma_p(\mathbf{v}_p)) - \xi \frac{\theta_s}{\nu_s} \phi_p (\mathbf{v}_p - \mathbf{v}_s) - \frac{\theta_p}{\nu_p} \nabla \mu_p = 0, \quad (4)$$

and

$$\nabla \cdot (\theta_s \sigma_s(\mathbf{v}_s)) - \xi \frac{\theta_s}{\nu_s} \phi_p (\mathbf{v}_s - \mathbf{v}_p) - \frac{\theta_s}{\nu_s} \sum_{j \geq 4} \hat{\phi}_j \nabla \mu_j - \frac{\theta_s}{\nu_s} \nabla \mu_s = 0, \quad (5)$$

where $\sigma_j(\mathbf{v}) = \frac{\eta_j}{2}(\nabla \mathbf{v}_j + \nabla \mathbf{v}_j^T) + \lambda_j I \nabla \cdot \mathbf{v}_j$ is the stress tensor ($\eta_j > 0$ and λ_j , $j = p, s$, are the viscosities), ξ_j are the drag coefficients, $\nu_p = (1 - \alpha)\nu_1 + \alpha\nu_2$ is the averaged polymer particle volume, $\theta_p = \theta_1 + \theta_2$, $\phi_s = \frac{n_s}{n_m + n_s}$, $\phi_p = \frac{n_m}{n_m + n_s}$, $\phi_j = \frac{n_j}{\sum_{i \neq 1,2} n_i}$ for $j \geq 4$ (assuming that the ions are dissolved in the solvent), are the polymer, solvent, and ion species per total solvent particle fractions, respectively. The third term in Eq. (5) represents the force that the solvent feels from the ion chemical potentials. The ion species satisfy the force balance equation

$$\xi_j n_j (\mathbf{v}_s - \mathbf{v}_j) - n_j \nabla \mu_j = 0, \quad j \geq 4. \quad (6)$$

In addition, if there is a free moving-edge to the gel, on one side of which (inside the gel) $\theta_p = \theta_p^-$, and on the other side of which (outside the gel) $\theta_p^+ = 0$, $\theta_s^+ = 1$, there are interface conditions,

$$\sigma_p(\mathbf{v}_p^-) \mathbf{n} = \frac{1}{\nu_p} \mu_p^- \mathbf{n}, \quad (7)$$

for the polymer,

$$(\sigma_s(\mathbf{v}_s^+) - \sigma_s(\mathbf{v}_s^-)) \mathbf{n} = \frac{1}{\nu_s} (\mu_s^+ - \mu_s^-) \mathbf{n}, \quad (8)$$

for the solvent, and

$$\mu_j^+ = \mu_j^-, \quad (9)$$

for the ion species, $j \geq 4$. \mathbf{n} is the normal to the free surface. The equations of motion and the interface conditions are derived using the standard variational arguments to minimize the rate of work, which constitutes the viscous rate of energy dissipated within the polymer and the solvent, energy dissipation rate due to the drag between solvent and polymer and between solvent and ion species particles as well as the rate of work required against the chemical potential, μ_j . Readers are directed to [19, 20, 21] to see the derivation details.

2.2 Chemical potential

The chemical potentials, μ_j , in Eq. (4, 5) are calculated via the Gibb's free energy

$$G = -k_B T S + U + P V, \quad (10)$$

where U is internal energy, S is entropy, T is temperature, k_B is Boltzmann's constant, P is pressure, and $V = \sum_j \nu_j n_j = \nu_1 n_1 + \nu_2 n_2 + \nu_s n_s$ is the total volume of the system (under

the assumption that the volume occupied by the ions are small compared to the monomer and solvent volumes). The chemical potential are

$$\mu_j = \frac{\partial G}{\partial n_j} = -k_B T \frac{\partial S}{\partial n_j} + \frac{\partial U}{\partial n_j} + \nu_j P = \mu_j^S + \mu_j^I + \nu_j P, \quad (11)$$

where μ_j^S , μ_j^I are the contribution due to entropy and internal energy respectively.

2.2.1 Entropic Contributions to Chemical Potentials

The entropy of the system is defined as

$$S = \sum N_i \omega_i, \quad (12)$$

where ω_i is the entropy per particle for the i^{th} particle. Using standard counting arguments [22], for single-molecule species,

$$\omega_j = -\ln(\phi_j) \quad j \geq 3 \quad (13)$$

The PEG and ChS chains exhibit permanent cross-linking bonds (i.e. covalent bonds), and the per-particle entropy is given by the rubber elasticity theory [23]

$$\omega_i = -\frac{3k_i}{2} \left[(\phi_i)^{-2/3} - 1 + \ln \phi_i \right], \quad i = 1, 2 \quad (14)$$

The particle fractions $\phi_1 = (1 - \alpha)\phi_p$ and $\phi_2 = \alpha\phi_p$, k_1, k_2 are the fraction representing the number of cross-linked monomers in one chain of PEG and ChS, respectively. The entropic part of the chemical potentials are

$$\begin{aligned} \frac{\mu_p^S}{k_B T} &= k_1 \phi_1^{-2/3} \left[\phi_1 + \frac{1 - \alpha}{2} \right] + k_2 \phi_2^{-2/3} \left[\phi_2 + \frac{\alpha}{2} \right] - \frac{3}{2} \left[k_2 \alpha (1 + \phi_2 \phi_s + \phi_2 \phi_s \ln \phi_2) + \right. \\ &\quad \left. k_1 (1 - \alpha) (1 + \phi_2 \phi_s + \phi_2 \phi_s \ln \phi_1) \right] - \phi_s \\ \frac{\mu_s^S}{k_B T} &= \ln \phi_s + \phi_p - k_1 \phi_1 (\phi_1^{-2/3} + 1) - k_2 \phi_2 (\phi_2^{-2/3} + 1) - \sigma_I \\ \frac{\mu_j^S}{k_B T} &= \ln \phi_j + 1 - \sigma_I, \end{aligned} \quad (15)$$

where $\sigma_I = \sum_{i \geq 4} \phi_j$ is the total ion particle fraction represents osmotic pressure as characterized by van't Hoff's law.

2.2.2 Internal Energy Contribution to Chemical Potentials

The internal energy consists of two contributions, long range electrostatic interactions and short range (nearest neighbor) interactions. The long range electrostatic interactions have energy

$$U_e = \sum_j z_j N_j \Phi_e, \quad (16)$$

where z_i is the charge on the i^{th} ionic species ($z_1 \equiv z_p$ is the average charge per monomer), and Φ_e is the electric potential.

To calculate the short range interaction energy for the polymer and solvent, we assume that for each of the $n_T (= n_m + n_s)$ particles have z neighboring interaction sites (called the coordination number). Of the total of n_m monomers, $k_1 n_1 = k_1(1 - \alpha)n_m$ and $k_2 n_2 = k_2 \alpha n_m$ of them are the cross-linked PEG and ChS pairs, respectively, and since the cross-linked particles are connected, we treat them as single species. The different species with their pairwise interactions (for either of the polymer species) are shown in Fig. 1. The cross-linked particle pairs have $2z-6$, $2z-4$ or $2z-5$ free interaction sites, depending on whether the monomers in the cross-linked pair are both in the middle of a polymer chain, both at the end of a chain, or have one monomer in the middle and the other at the end of a polymer chain, respectively (Fig. 1a,b,c). An uncross-linked monomer has either $z-2$ or $z-1$ free interaction sites, based on its position in the polymer chain (Fig. 1d,e), while the solvent particles have z free interaction sites (Fig. 1f).

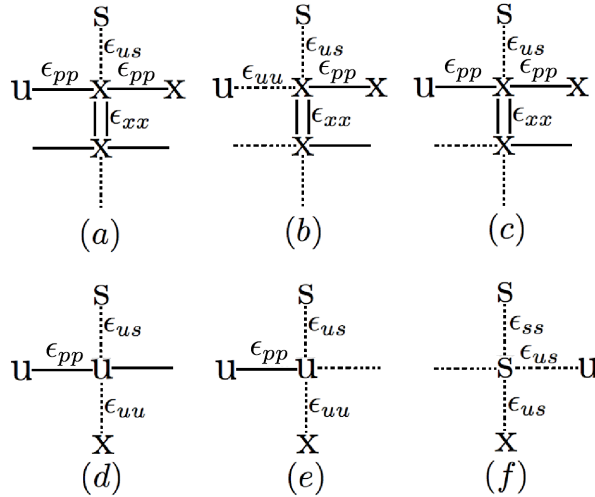


Figure 1: Pairwise interactions of the different species and their associated interaction energies for: (a)-(c) cross-linked monomers, x, (d) and (e) uncross-linked monomers, u, and (f) solvent, s. Double solid lines denote cross-linking, single solid lines denote interactions within a polymer chain while the other types of interactions are denoted by dashed lines. The nearest neighbor interactions are assumed identical for both the PEG and ChS monomer species.

We let $k_B T_0 \epsilon_{xx}$, $k_B T_0 \epsilon_{uu}$, $k_B T_0 \epsilon_{pp}$, $k_B T_0 \epsilon_{us}$ and $k_B T_0 \epsilon_{ss}$ be the interaction energy associated with the covalent cross-links, uncross-linked monomer-monomer interaction (with the assumption that the different types of monomers have the same interaction energy), monomer-monomer interaction within a polymer strand, monomer-solvent interaction and solvent-solvent interaction, respectively. These interactions are assumed identically equal for both PEG and ChS monomers. T_0 is a reference temperature. The interaction energies for the different species of polymer and solvent particles, calculated using standard mean-field

arguments, are

$$\frac{F_x^1}{k_B T_0} = r \left(\frac{k_1 N_1 - 2}{k_1 N_1} \right) \left(\frac{k_2 N_2 - 2}{k_2 N_2} \right) n_m (2\epsilon_{xx} + (2z - 6)E_{us} + 4\epsilon_{pp}), \quad (17)$$

$$\frac{F_x^2}{k_B T_0} = r \left(\frac{2}{k_1 N_1} \right) \left(\frac{2}{k_2 N_2} \right) n_m (2\epsilon_{xx} + (2z - 4)E_{us} + 2\epsilon_{pp}), \quad (18)$$

$$\frac{F_x^3}{k_B T_0} = r \left(\frac{2}{k_1 N_1} \frac{k_2 N_2 - 2}{k_2 N_2} + \frac{2}{k_2 N_2} \frac{k_1 N_1 - 2}{k_1 N_1} \right) n_m (2\epsilon_{xx} + (2z - 5)E_{us} + 3\epsilon_{pp}), \quad (19)$$

$$\frac{F_u^1}{k_B T_0} = \left((1 - k_1)(1 - \alpha) \frac{k_1 N_1 - 2}{k_1 N_1} + (1 - k_2)\alpha \frac{k_2 N_2 - 2}{k_2 N_2} \right) n_m ((z - 2)E_{us} + 2\epsilon_{pp}), \quad (20)$$

$$\frac{F_u^2}{k_B T_0} = \left((1 - k_1)(1 - \alpha) \frac{2}{k_1 N_1} + (1 - k_2)\alpha \frac{2}{k_2 N_2} \right) n_m ((z - 1)E_{us} + \epsilon_{pp}), \quad (21)$$

$$\frac{F_s}{k_B T_0} = z n_s \left(\epsilon_{us} \frac{N_m}{N_T} + \epsilon_{ss} \frac{N_s}{N_T} \right), \quad (22)$$

respectively, where $r = \frac{k_1(1-\alpha)+k_2\alpha}{2}$ and $E_{us} = \epsilon_{uu} \frac{n_m}{n_T} + \epsilon_{us} \frac{n_s}{n_T}$. The total per particle interaction energy is

$$\begin{aligned} U^I &= \frac{1}{2(n_m + n_s)} (F_x^1 + F_x^2 + F_x^3 + F_u^1 + F_u^2 + F_s) \\ &= k_B T_0 \left[\chi \phi_p \phi_s + \mu_0^s \phi_s + \mu_0^p \phi_p + \frac{z}{2} \epsilon_{us} \right], \end{aligned} \quad (23)$$

where

$$\begin{aligned} \chi &= \frac{z}{2}(\epsilon_1 + \epsilon_2) - \left(r + 1 + \frac{k_1(1 - \alpha) - k_2\alpha - 2(1 - \alpha)}{2k_1 N_1} + \frac{k_2\alpha - k_1(1 - \alpha) - 2\alpha}{2k_2 N_2} \right) \epsilon_1, \\ \mu_0^p &= r\epsilon_3 - \frac{z}{2}\epsilon_1 + \left(1 + \frac{k_1(1 - \alpha) - k_2\alpha - 2(1 - \alpha)}{2k_1 N_1} + \frac{k_2\alpha - k_1(1 - \alpha) - 2\alpha}{2k_2 N_2} \right) \epsilon_4, \\ \mu_0^s &= -\epsilon_2 \frac{z}{2}, \end{aligned} \quad (24)$$

and

$$\epsilon_1 = \epsilon_{us} - \epsilon_{uu}, \quad \epsilon_2 = \epsilon_{us} - \epsilon_{ss}, \quad \epsilon_3 = \epsilon_{xx} - \epsilon_{uu}, \quad \epsilon_4 = \epsilon_{pp} - \epsilon_{uu}. \quad (25)$$

In polymer chemistry literature, the coefficients, χ, μ_0^p, μ_0^s , are referred as the Flory interaction parameter and the chemical potentials of pure polymer and solvent species respectively [24]. The factor $\frac{1}{2}$ in the per-particle interaction energy (Eqn. 23) is to correct for double counting. The corresponding contributions to chemical potentials are

$$\mu_p^I = k_B T_0 (\chi \phi_s^2 + \mu_p^0), \quad \mu_s^I = k_B T_0 (\chi \phi_p^2 + \mu_s^0). \quad (26)$$

In summary, the chemical potential for the polymer and solvent phase is

$$\frac{\mu_j}{k_B T} = M_i + z_i \Psi_e + \nu_i \frac{P}{k_B T}, \quad j = p, s, \quad (27)$$

where $\Psi_e = \frac{\Phi_e}{k_B T}$, $M_p = \frac{1}{k_B T}(\mu_p^S + \mu_p^I)$ and $M_s = \frac{1}{k_B T}(\mu_s^S + \mu_s^I) + \sigma_I$. The functions M_i are chosen so as to highlight the contribution of the various terms in the net swelling pressure (see Eq. (31) later). For the ion species, $\mu_j^I = 0$, and we ignore its volume, ν_j , so that

$$\frac{\mu_j}{k_B T} = \ln \phi_j + 1 - \sigma_I + z_j \Psi_e, \quad j \geq 3, \quad (28)$$

Finally, the gel-sol interface conditions, Eqns. (7-8), become

$$\begin{aligned} \sigma_p(\mathbf{v}_p^-) \mathbf{n} &= \frac{k_B T}{\nu_p} \left(M_p^- + z_p \Psi_e + \nu_p \frac{P}{k_B T} \right) \mathbf{n}, \\ (\sigma_s(\mathbf{v}_s^+) - \sigma_s(\mathbf{v}_s^-)) \mathbf{n} &= \frac{k_B T}{\nu_s} \left(M_s^+ - M_s^- - \sigma_I^+ + \sigma_I^- - \nu_s \frac{P}{k_B T} \right) \mathbf{n}, \end{aligned} \quad (29)$$

where $P \equiv P^-$, $P^+ = 0$ and $\Psi_e^- \equiv \Psi_e$, $\Psi_e^+ = 0$. Eliminating P from these we find the single interface condition

$$(\sigma_p(\mathbf{v}_p^-) - \sigma_s(\mathbf{v}_s^-) + \sigma_s(\mathbf{v}_s^+)) \mathbf{n} = \Sigma_{net} \mathbf{n}, \quad (30)$$

where Σ_{net} is the net swelling pressure,

$$\frac{\Sigma_{net}}{k_B T} = \frac{M_p^-}{\nu_p} - \frac{M_s^-}{\nu_s} + \frac{T_0 \mu_s^0}{T \nu_s} + \frac{z_p \Psi_e}{\nu_p} + \frac{\sigma_I^-}{\nu_s} - \frac{\sigma_I^+}{\nu_s}. \quad (31)$$

The term $(z_p \Psi_e)$ represents the Donnan swelling pressure while $(\sigma_I^- - \sigma_I^+)$ represents the Osmotic pressure due to the ions dissolved in the solvent (also termed as the ‘Net Osmolarity’ inside the gel).

2.3 Ionized-species chemistry

Let the concentrations per total volume of the polymer species be denoted by $m = [M^{2-}]$, $y = [MH^-]$, $v = [MNa^-]$, $w = [MH_2]$, $x = [MNa_2]$, $q = [MHN a]$, with the total monomer concentration

$$m_T = m + y + v + w + x + q, \quad (32)$$

and the ChS-monomer volume fraction $\theta_2 = \nu_2 N_A m_T$. The charged ChS monomer concentration, m , is obtained from Eqn. (32). The concentrations per solvent volume of the ion species are denoted as $n = [Na^+]$, $h = [H^+]$, and $c_l = [Cl^-]$. With concentrations expressed in units of moles per liter, the relationship between ion particle fractions ϕ_j and concentrations c_j is $\phi_j = \nu_s N_A c_j$, where N_A is Avagadro’s number. Under the assumption of fast chemistry, the law of mass action for the monomer binding reactions (Eq.(1)) reduces to

$$\begin{aligned} (a) \quad & k_h m h \theta_s + (k_{-h_2} w + k_{-hn} q) \phi_s^2 = k_{-h} y \phi_s^2 + (k_{h_2} y h + k_{hn} y n) \theta_s \\ (b) \quad & (k_n m n + k_{n_2} v n) \theta_s = (k_{-n} v + k_{-n_2} x) \phi_s^2 \\ (c) \quad & k_{h_2} y h \theta_s = k_{-h_2} w \phi_s^2 \\ (d) \quad & k_{n_2} v n \theta_s = k_{-n_2} x \phi_s^2 \\ (e) \quad & k_{hn} y n \theta_s = k_{-hn} q \phi_s^2 \end{aligned} \quad (33)$$

Since the unbinding (dissociation) reactions are ionization reactions that require two “units” of solvent, we take the unbinding reaction rates to be $k_{-C}\phi_s^2$, $C = h, n, h_2, n_2, hn$, and because ChS monomers carry a double negative charge, $2k_{i_2} = k_i, k_{-i_2} = 2k_{-i}$, $i = n, h$ and $4k_{hn} = k_h + k_n, k_{-hn} = k_{-h} + k_{-n}$. Simplifying Eq. (33),

$$y = \frac{\theta_s}{K_h\phi_s^2}mh, \quad v = \frac{\theta_s}{K_n\phi_s^2}mn, \quad w = \left(\frac{\theta_s}{2K_h\phi_s^2}\right)^2 mh^2, \quad x = \left(\frac{\theta_s}{2K_n\phi_s^2}\right)^2 mn^2, \quad q = \left(\frac{\theta_s}{\sqrt{K_h K_{hn}}\phi_s^2}\right)^2 mhn, \quad (34)$$

where $K_h = \frac{k_{-h}}{k_h}$, $K_n = \frac{k_{-n}}{k_n}$, $K_{h_2} = 4K_h$, $K_{n_2} = 4K_n$ and $K_{hn} = 4\frac{k_{-h}+k_{-n}}{k_h+k_n}$.

Similarly, when the diffusion of the ion species and their binding and unbinding reactions are fast compared to the swelling kinetics of the polymer network, the Nernst-Planck equation, describing the ion movement (together with the interface conditions Eq.(9)), reduces to

$$C = C_b e^{-z_C \Psi_e} \quad (35)$$

with $C = h, n, c_l$, $z_n = z_h = 1$ and $z_{c_l} = -1$ and the subscript ‘b’ denotes the corresponding bath concentrations. The electrostatic potential, Ψ_e , is determined by the electroneutrality constraint inside the gel,

$$(n + h - c_l)\theta_s + z_p m_T = 0, \quad (36)$$

where z_p is the average charge per ChS-monomer. The electro-neutrality in the bath requires (i.e. setting $\Psi_e = 0$ in Eqn. 35 and then using Eqn. 36)

$$n_b + h_b - c_{lb} = 0, \quad (37)$$

The average charge, z_p , depends on the residual charge of the bound ChS-polymer species,

$$z_p m_T = -(2m + y + v). \quad (38)$$

The system of equations including the mass conservation Eqn. (2), total volume conservation Eqn. (3) together with force balance Eqns. (4-5) and interface condition Eqn. (30), subject to the constraints Eqn. (32) (monomer conservation), Eqn. (35) (ion motion) and Eqn. (36) (electroneutrality); completely describes the dynamical motion of a freely swelling gel. Finally, the ‘Net-Osmolarity’ in the gel, Osm , is

$$\text{Osm} = (n + h + c_l) - (n_b + h_b + c_{lb}) = (n_b + h_b)(e^{-\Psi_e} + e^{\Psi_e} - 2), \quad (39)$$

which measure the excess moles of solute (inside the gel) per liter of solvent.

3 Material and methods

Poly(ethylene glycol) dimethacrylate (PEGDM) was synthesized via microwave methacrylation [25] by reacting poly(ethylene glycol) (Mol. wt. 4600 g/mol) with methacrylic anhydride in the presence of hydroquinone (Sigma-Aldrich). The PEGDM product was recovered by dissolving the mixture in methylene chloride followed by precipitation with ethyl ether, filtration and drying. The degree of methacrylation was determined to be 85% by $^1\text{HNMR}$ (Varian

VYR-500). Methacrylated chondroitin sulfate (ChSMA) was synthesized as described previously [18] by reacting chondroitin sulfate A (Sigma-Aldrich) in a 1:8 ratio with methacrylic anhydride in deionized water (DI-H₂O) at 4°C and a pH of 8 for 24 hours. The product was recovered by precipitation in chilled methanol and dialyzed in DI-H₂O overnight. The purified product was recovered via lyophilization and the degree of methacrylation was determined to be 16% by ¹HNMR (Varian VYR-500), indicating that there were 16 methacrylates per ChSMA molecule.

Ionic gels were formed by co-polymerizing PEGDM macromers with ChSMA macromers at a final macromer concentration of 10 % (g/g) with 0.05% (g/g) photoinitiator Irgacure 2959 (Ciba Specialty Chemicals) in deionized water (DI-H₂O). The macromer solution was placed in between two glass slides with a 1 mm spacer and exposed to 365 nm light with an intensity of 5 mW cm² for ten minutes. The ratio of PEGDM:ChSMA in the macromer solution was varied as follows: 90:10, 80:20, 70:30, 60:40 and 50:50 by weight. After polymerization, cylindrical gels were punched out using a 5 mm diameter biopsy punch and immediately weighed before being put into a solution and allowed to swell. The gels were then placed in the solution of interest to investigate the effect of salt concentration and pH on the swelling of the PEGDM:ChSMA gels. In a separate experiment, a subset of gels was placed in DI-H₂O for 48 hours and the soluble fraction of the ChSMA (i.e., the fraction not incorporated into the gel) was assessed using the DMMB dye assay [26]. It was confirmed that 99% of the ChSMA was incorporated into the gel.

Gel swelling in electrolyte solutions of varying concentrations of NaCl in DI-H₂O was investigated. Solutions were prepared of 0.1 mM, 1 mM, 10 mM, 0.1M, and 1 M NaCl while the pH was maintained at pH 7. The gels were placed into each solution after the initial mass was taken and allowed to swell for 48 hours. Gel mass was measured at various time points throughout the 48 hours to ensure that gels had reached their equilibrium swelling by 48 hours. The effect of pH on the swelling of PEGDM:ChSMA gels was also explored. These gels were placed in various pH solutions, which were prepared using 1M NaOH and 1M HCl in DI water. The pH of the solvents varied from pH 3 to pH 8. An initial mass of the gel was taken for a 5-mm disk immediately after polymerization. Gels were placed in the solution of interest and mass measured at various time points up to 48 hours to ensure equilibrium swelling was reached.

The initial volume of the dry polymer, V_i , was determined from the initial mass, m_i , using a weighted density of the ChSMA, PEGDM, and DI-H₂O, as follows

$$V_i = 0.1 \left(\frac{m_i \cdot \%PEGDM}{\rho_{PEGDM}} + \frac{m_i \cdot \%ChSMA}{\rho_{ChSMA}} \right) \quad (40)$$

The mass of the gel at equilibrium was measured and used to determine the swollen volume $V_{swollen}$. It was assumed that all polymer was incorporated in the gel, which was confirmed for chondroitin sulfate, and therefore a change in mass was solely due to the a change in the water content. Hence

$$V_{swollen} = 0.1 \left(\frac{m_i \cdot \%PEGDM}{\rho_{PEGDM}} + \frac{m_i \cdot \%ChSMA}{\rho_{ChSMA}} \right) + \frac{m_{swollen} - 10\%m_i}{\rho_{solvent}} \quad (41)$$

The percent of PEGDM and ChSMA was dependent on the ratio of PEGDM:ChSMA which varied from 90:10 to 50:50. The initial mass, m_i , was the mass of the gel immediately

following polymerization and before being placed in a solvent. The swollen mass, $m_{swollen}$, is the mass of the gel at equilibrium. The density of the PEGDM, ρ_{PEGDM} , was estimated to be 1.07 g/ml and the density of the ChSMA, ρ_{ChSMA} , was assumed to be 1.001 g/ml [27]. The density of the solvents, $\rho_{solvent}$, was assumed to be 1.00 g/ml. The volume fraction of the polymer was calculated as the volume of the dry polymer (i.e. before swelling) divided by the volume of the swollen gel, $V_i/V_{swollen}$.

4 Results and discussion

At equilibrium, we solve the system of equations given by the interface conditions (Eqn. 30), monomer conservation (Eqn. 32), ion motion (Eqn. 35) and electroneutrality (Eqn. 36). The mass, volume and the force balance (Eqns. 2-5) are trivially satisfied. The values of the parameter used in our numerical calculations are listed in Table 1. The constants in the model are the monomer volumes, ν_1, ν_2 , the number of nearest neighbor in the PEG-ChS polymer lattice, z , and the nearest neighbor interaction energies, ϵ_i , assumed identically equal for both types of polymer (eqn.25). The undetermined constants are the binding affinities of the various cations with the gel, K_h, K_n (eq.33).

The monomer volumes are found from the density and the molecular weight information ($\nu_i = M_i/(\rho_i * N_A)$). The cross-linked PEG-ChS matrix has a 3-D configuration, which suggests that we choose the coordination number, $z = 6$, hence mimicking a 3-D cubic lattice. The interaction energies are found from the solubility data, δ_i , and the standard free energies, $k_B T_0 \mu_p^0$ and $k_B T_0 \mu_s^0$ (eqn.23). The standard free energy, is the energy of all the interactions between the molecule and its neighbors in a pure state that have to be disrupted to remove the molecule from the pure state [29] (pg.141-144). These can be determined from the Hildebrand solubility parameters, δ_i , via

$$\begin{aligned} -k_B T_0 \mu_p^0(\alpha = 0) &= \nu_1 \delta_1^2 \\ -k_B T_0 \mu_p^0(\alpha = 1) &= \nu_2 \delta_2^2 \\ -k_B T_0 \mu_s^0 &= \nu_w \delta_w^2, \end{aligned} \quad (42)$$

where ν_w is the volume of 1 molecule of water. The negative sign in eqn.42 indicates that $k_B T_0 \mu_p^0, k_B T_0 \mu_s^0 < 0$, since they are the interaction energies. For example, at $T_0 = 298K$, $\nu_w = 2 \times 10^{-23} \text{ cm}^3$ as the monomeric volume of 1 water molecule and the solubility parameter $\delta_w = 48.07 MPa^{1/2}$, the non-dimensional parameter, μ_s^0 (from eq.23), is

$$\mu_s^0 = -\epsilon_2 \frac{z}{2} = -\nu_m \delta^2 / (k_B T_0) = -11.23, \quad (43)$$

giving the value of the interaction energy, $\epsilon_2 = 3.74$.

4.1 Parameter estimation

The experimental data are used to calibrate the model for the gel volume-fraction at equilibrium [18]. Fig 2 presents the sample averaged equilibrium data-points at different salt concentrations and neutral pH (Fig 2a) and at variable pH solution (Fig 2b). The equilibrium values were noted at time $t = 48$ hrs. Each point represents the average of four samples,

	PEG ($i = 1$)	ChS ($i = 2$)	Units	Source
Density (ρ_i)	1.07	1.001	g/mL	[18, 27]
Molecular weight (M_i)	4600	48700	g/mol	[28]
Repeat unit per chain (N_i)	102	86	–	[28]
Cross-link fraction (k_i)	0.25, 0.5, 0.75	0.25, 0.35, 0.45	–	[17]
Hildebrand solubility (δ_i)	17.39	5.19	MPa ^{1/2}	[29]
Hildebrand solubility for water (δ_w)		48.07	MPa ^{1/2}	[29]

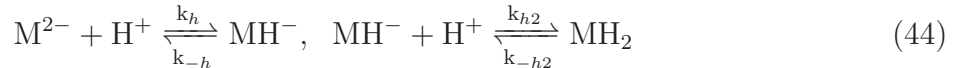
Table 1: Parameters common to all the numerical results. The reference temperature for the solubility parameters is fixed at $T_0 = 298\text{K}$.

with values noted in identical conditions, with the upper and the lower limits in the error bar representing maximum and the minimum variation from the average, respectively.

The molecular mass and the density of PEG were fixed at 4600 g/mol and 1.07 g/mL, while that of ChS were fixed at 48700 g/mol and 1.001 g/mL, respectively. These values give the monomer volumes of the PEG chains as $\nu_1 = 7.14 \times 10^{-21} \text{ cm}^3$, and that of ChS chains as $\nu_2 = 8.08 \times 10^{-20} \text{ cm}^3$. The Hildebrand solubility parameters for pure species (values given in Table 1) and the monomer volumes are used to calculate the interaction energies, ϵ_i ($i=1,\dots,4$). Using the relations in Eqn. (42), these values are fixed at $\epsilon_1 = 0.0$, $\epsilon_2 = 3.74$, $\epsilon_3 = 9.58$, $\epsilon_4 = -56.17$. The reference temperature is fixed at $T_0 = 298\text{K}$, while experiments were performed at $T = 293\text{K}$. The undetermined parameters, namely the binding affinities, K_h , K_n (Eqn.33) are computed by constructing a nonlinear least-square function and employing the conventional subspace trust region method implemented in Matlabs **lsqnonlin** [30]. These values are found as $\log_{10}(K_n) = -2.51$, $\log_{10}(K_h) = -3.56$. It is observed that the cross-link fraction of these gels is variable under identical experimental conditions. Therefore, we study the effect of cross-linking on the equilibrium configuration by selecting 3 different pairs of cross-link fractions for the PEG-ChS gels: CL₁: (0.25, 0.25), CL₂: (0.5, 0.35) and CL₃: (0.75, 0.45). The solid lines (in Fig. 2) are the equilibrium values predicted by the model.

4.2 Effects of changes in the gel composition

Fig. 3a,b,c depict the equilibrium volume fraction, corresponding Donnan pressure and the net-osmolarity, respectively, vs. the weight-fraction α , of the charged component of the gel (i.e. ChS) and for different wt/vol percentages. The gel is dissolved in salt-free, neutral water ($[H]_b = 10^{-7} \text{ M}$), and the negative charges on the gel causes water to dissociate into hydrogen and hydronium ions. H^+ ions can then bind with the monomers with the binding reaction



A chondroitin sulfate-dominant gel solution swells (i.e. θ_p decreases vs. α , Fig. 2a), and has a higher osmolarity at equilibrium (i.e. $|\text{Osm}|$ increases vs. α , Fig. 2b). This is because the swelling is driven by Donnan pressure (Fig. 3b) as well as the osmotic pressure (Fig. 3c) which is non-negligible in a charged gel. The negative charges on the gel causes water to furnish H^+ ions which contributes to a non-zero ionic difference (or ‘Net Osmolarity’) across the gel. Similarly, gels with a higher cross-link fraction prefer a de-swelled equilibrium state

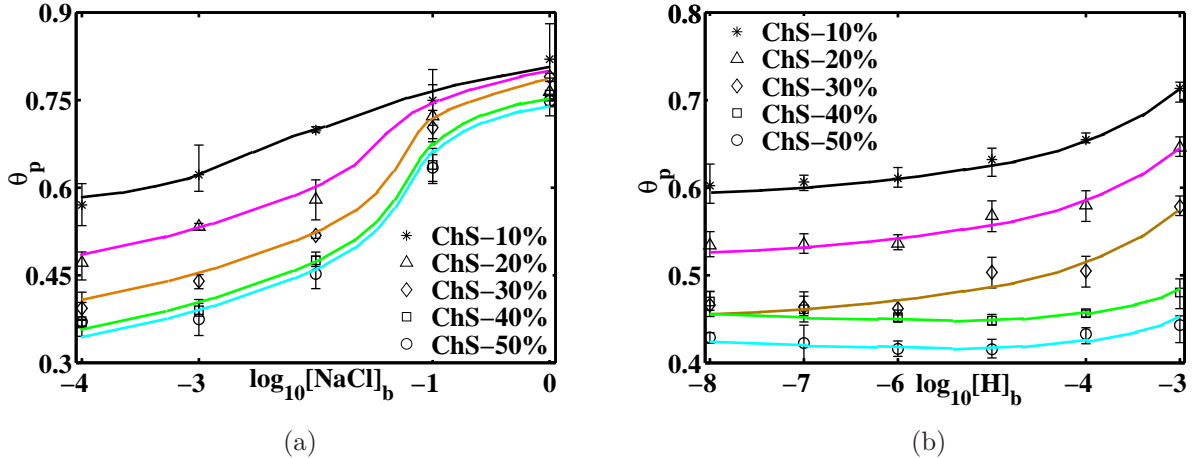


Figure 2: Experimental data of equilibrium volume-fraction of the PEG-ChS gel vs. (a) different NaCl concentration in the bath (in mol/l) and pH = 7.0, and (b) different pH and zero salt concentration. The sample is a 10 wt% gel. The molecular mass and the density of PEG 4600 g/mol and 1.07 g/mL, while that of ChS is 48700 g/mol and 1.001 g/mL, respectively. The experiments were performed at a constant room temperature of 293K. The solid lines correspond to the volume fraction values predicted by the model.

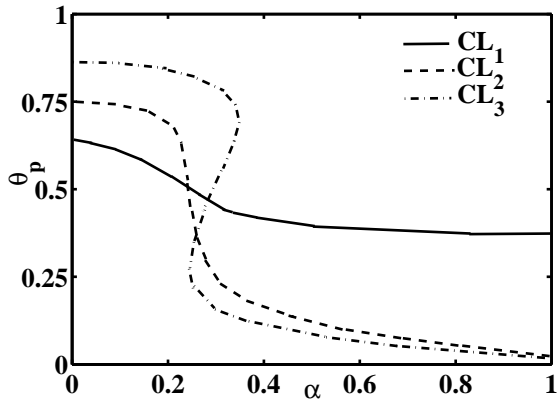
at low ChS weight fractions and then exhibit a more prominent swelling at higher ChS weight fractions (for e.g., compare the swelling profile of the case CL₃ versus the case CL₁, in the range $\alpha < 0.25$, and $\alpha > 0.40$, respectively, Fig. 3a). Experiments corroborate that a highly cross-linked network provides a barrier against the Donnan pressure and hence acts against swelling [9].

4.3 Effects of changes in the bath salt concentration

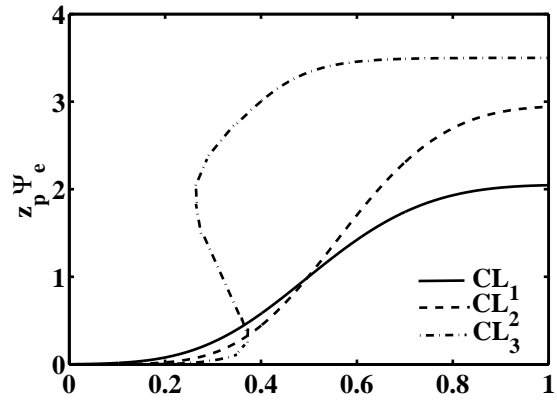
Next we explore the situation in which the gel is immersed in an infinite bath, with fixed hydrogen concentration ($H_b = 10^{-7}$ M), containing a monovalent ion, e.g., Na⁺. Both hydrogen and sodium ions compete to bind with the negatively charged gel and the list of binding reactions are given in Eqn. (1). Fig. 4a,b,c highlight the equilibrium volume fraction, Donnan pressure and the net-osmolarity vs. the bath salt concentration, $[\text{NaCl}]_b$, respectively, for gels with different cross-link fractions but a fixed 10% ChS composition (by weight) out of the total polymer weight.

A higher salt concentration promotes gel de-swelling (e.g. consider volume fraction values at $[\text{NaCl}]_b=1$ M vs. those at $[\text{NaCl}]_b = 10^{-3}$ M, Fig. 4a). A high salt concentration implies that more Na⁺ ions are available to bind with the gel, thereby reducing the Donnan swelling pressure. Although the osmotic pressure increases at high salt concentrations (Fig. 4c), it is the Donnan pressure that dominates the swelling mechanism in this case.

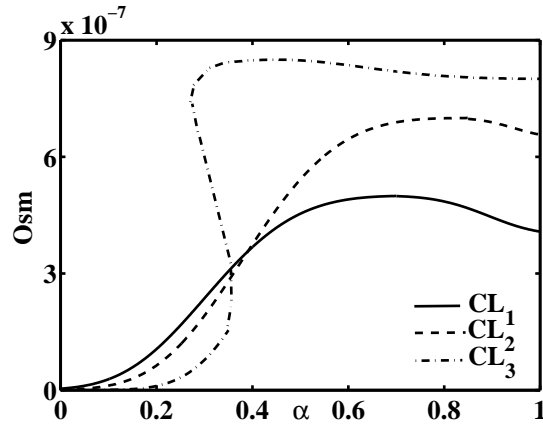
At lower salt concentrations, however, swelling is insignificant (i.e. $\theta_p \approx 0.55$ for concentrations $[\text{NaCl}]_b < 10^{-6}$ M). At these low concentrations water breaks down to produce H⁺ ions to bind with the gel, which keeps the Donnan pressure relatively fixed (i.e. $z_p \Psi_e \approx 10$ for $[\text{NaCl}]_b < 10^{-6}$ M, Fig. 4b) and the osmotic pressure is nearly zero (Fig. 4c). Gels



(a)



(b)



(c)

Figure 3: (a) Equilibrium polymer volume-fraction, (b) Donnan swelling pressure, and (c) Net-Osmolarity, vs. α , the fraction of Chondroitin sulfate component for gel solutions with different cross-link fractions.

with higher cross-link fractions provide greater resistance against the Donnan pressure and therefore prefer a de-swelled state (i.e. compare the volume fraction values for the different curves in Fig. 4a).

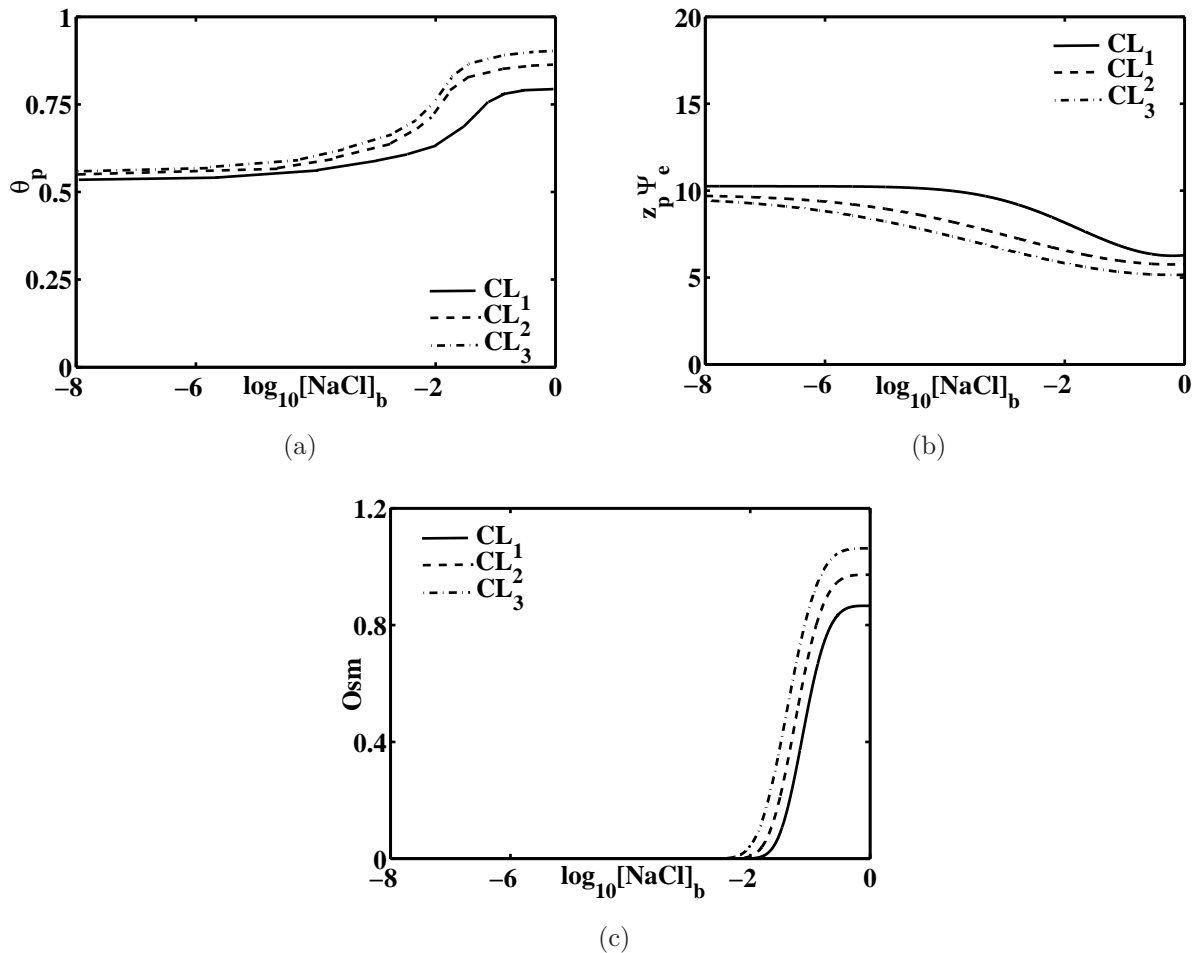


Figure 4: (a) Equilibrium polymer volume-fraction, (b) Donnan swelling pressure, and (c) Net-Osmolarity, vs. NaCl-concentration (in mol/lit.) in the bath. Different curves represent samples with a fixed 10% ChS weight percent, but with a variable cross-link fraction.

Fig. 5a,b show the equilibrium swelling-deswelling state and the net-osmolarity vs. the bath salt concentration, respectively, for gels with variable ChS weight percentage but the cross-link fraction fixed at $k_1 = 0.25$, $k_2 = 0.25$. Once again, at high salt concentrations the gel de-swells (Fig. 5a). This is due to the lowering of average charge per monomer and hence the Donnan pressure, the driving mechanism for gel swelling. Comparing the different curves in Fig. 5a, we find that higher weight percentages of ChS result in higher average charge per monomer which leads to gel-swelling, driven by the Donnan pressure as well as the osmotic pressure (Fig. 5b).

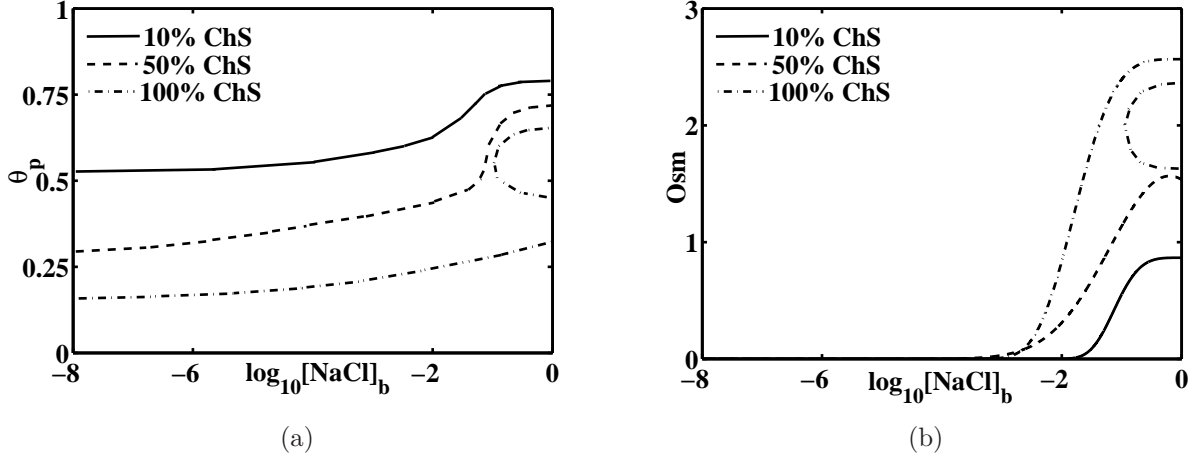


Figure 5: (a) Equilibrium polymer volume-fraction, and (b) Net-Osmolarity, vs. NaCl-concentration (in mol/lit.) in the bath. Different curves represent gel samples with a fixed cross-link fraction, $k_1 = 0.25$, $k_2 = 0.25$, and with a variable ChS weight percentage.

4.4 Effects of changes in the bath pH

Finally, we predict the equilibrium configuration (Fig. 6a) and the net osmolarity (Fig. 6b) of gels (the cross-link fraction fixed at $k_1 = 0.25$, $k_2 = 0.25$ and variable ChS weight percent) immersed in salt-free, acidic/basic solution. The binding reactions of the charged polymer with the ions are those given in Eqn. (44). In a variable acidic conditions (e.g. $\log_{10}H^+ > -1.9$), the gel de-swells sharply either via a continuous / reversible transition (i.e. referring to the changes in the 10% and 50% ChS-curves) or discontinuous / irreversible jump (for pure ChS polymers). These transitions highlight a non-linear swelling/de-swelling response mechanism of the ionic gels with respect to the pH variations in salt-free solution.

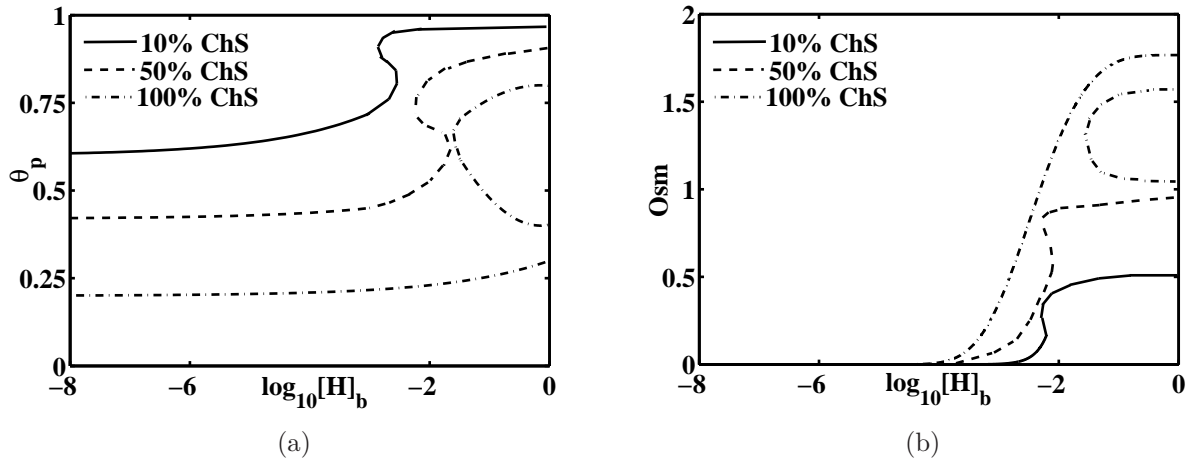


Figure 6: (a) Equilibrium polymer volume-fraction, and (b) Net-Osmolarity, vs. bath pH, for a fixed 10% wt/vol gel.

5 Conclusions

In this paper, we have developed a multi-phase, multi-species model to quantify the swelling/de-swelling mechanism for polyelectrolyte gels. Using this model we have quantified the effects of the changes in bath concentration of monovalent solute (i.e. [NaCl]), the average charge per monomer (via variations in the chondroitin sulfate mass percentage) and the cross-link fraction of the gel on the equilibrium swelled/de-swelled configuration. We learned that, generally speaking, increasing the bath concentration of the ion species as well as the cross-link fraction of the gels per volume of total solution leads to deswelling while increasing the average charge per monomer leads to swelling, in agreement with experimental observations [17, 18, 28]. However, because of complex interactions between competing forces (e.g. Donnan forces which aids swelling and the elastic forces from covalent cross-links which helps de-swelling), the swelling/de-swelling mechanism is non-linear (or hysteretic) exhibiting a first order (or discontinuous) transition or a second order (or continuous) transition in many situations. A change in the solute concentration leads to changes in the equilibrium swelling of the gel which is either irreversible (in the case for first order transition) or reversible (for second order transitions). The full study of the kinetics of swelling these gels under spatio-temporally varying mechanical loads will be the subject of a forthcoming article.

Acknowledgement: This work was supported in part by grants NSF CAREER 0847390. The authors would also like to thank Dr. James P. Keener (Department of Mathematics, University of Utah) for providing for providing useful insights at various stages of model development.

References

- [1] Mow V.C. and Ratcliffe A., ‘Structure and function of articular cartilage and meniscus’, *Basic Ortho. Biomech. 2nd ed.* 11377 (1997).
- [2] Mow V.C., Ateshian G.A., Spilker R.L., ‘Biomechanics of diarthrodial joints: a review of twenty years of progress’, *J. Biomech. Eng.* **115**, 46067 (1993).
- [3] Armstrong C.G. and Mow V.C., ‘Variations in the intrinsic mechanical properties of human articular cartilage with age, degeneration, and water content’, *J. Bone Joint Surg. Am.*, **64**, 88-94 (1982).
- [4] Maroudas A., ‘Physicochemical properties of articular cartilage’ *Adult Articular Cartilage, 2nd ed.* 215323 (1979).
- [5] Setton L.A., Zhu W. and Mow V.C. ‘The biphasic poroviscoelastic behavior of articular cartilage: role of the surface zone in governing the compressive behavior’ *J. Biomech.* **26** 58192 (1993).
- [6] Maroudas A., Wachtel E., Grushko G., Katz E. P. and Weinberg P. ‘The effect of osmotic and mechanical pressures on water partitioning in articular cartilage’, *Biochim. Biophys. Acta* **1073** 28594 (1991).

- [7] Maroudas A. ‘Physicochemical properties of cartilage in the light of ion exchange theory’, *Biophys. J.* **8** 575-95 (1968).
- [8] Donnan F. G., ‘The theory of membrane equilibria’, *Chem. Rev.*, **1** 73-90 (1924).
- [9] Muir H., Bullough P. and Maroudas A., ‘The distribution of collagen in human articular cartilage with some of its physiological implications’ *J. Bone Joint Surg. Br.* **52** 554-63 (1970).
- [10] Tanaka T., Filmore D., Sun S.T., Nishio I., Swislow G. and Saha A., ‘Phase transition in ionic gels’, *Phys. Rev. Lett.* **45**(20), 1636 (1980).
- [11] English A.E., Mafe S., Manzanares J., Yu X., Grosberg A.Y. and Tanaka T., ‘Equilibrium swelling properties of polyampholytic hydrogels’, *J. Chem. Phys.* **104** 8713-8720 (1996).
- [12] Wolgemuth C., Mogilner A. and Oster G., ‘The hydration dynamics of polyelectrolyte gels with applications to cell motility and drug delivery’, *Eur. Biophys. J.* **33**, 146-158 (2004).
- [13] De, S.K., Aluru, N.R., Johnson, B., Crone, W.C., Beebe, D.J., Moore, J., ‘Equilibrium swelling and kinetics of pH-responsive hydrogels: models, experiments, and simulations’, *J. Microelectromech. Syst.* **11**, 544-555 (2002).
- [14] Kokufuta E., ‘Polyelectrolyte Gel Transitions: Experimental Aspects of Charge Inhomogeneity in the Swelling and Segmental Attractions in the Shrinking’, *Langmuir* **21**(22) 10004-10015 (2005).
- [15] Hirotsu S., ‘Softening of bulk modulus and negative Poissons ratio near the volume phase transition of polymer gels’, *J. Chem. Phys.* **94**, 3949 (1991).
- [16] Zribi O.V., Kyung H., Golestanian R., Liverpool T.B. and Wong G.C.L., ‘Condensation of DNA-actin polyelectrolyte mixtures driven by ions of different valences’, *Phys. Rev. E* **73**, 031911 (2006).
- [17] Bryant S. J. and Anseth K. S., ‘Controlling the spatial distribution of ECM components in degradable PEG hydrogels for tissue engineering cartilage’, *J. Biomed. Mat. Res.* **64**(1), 70-9 (2003).
- [18] Bryant S. J., Davis-Arehart K. A., Luo N., Shoemaker R. K., Aurther J. A. and Anseth K. S., ‘Synthesis and characterization of photopolymerized multifunctional hydrogels: water soluble poly(vinyl alcohol) and chondroitin sulfate macromers for chondrocyte encapsulation’, *Macromolecules*, **36**(7), 2556-62 (2004).
- [19] J. P. Keener, S. Sircar and A. Fogelson, Kinetics of swelling gels, *SIAM J. Appl. Math.*, **71**(3) 854-875 (2011).
- [20] J. P. Keener, S. Sircar and A. Fogelson, Influence of free energy on swelling kinetics of gels, *Phy. Rev. E*, **83**(4) 041802 (2011).

- [21] S. Sircar, J. P. Keener and A.L. Fogelson, ‘The effect of divalent vs. monovalent ions on the swelling of Mucin-like polyelectrolyte gels: Governing equations and equilibrium analysis’, *J. Chem. Phys.*, **138** 014901 (2013).
- [22] M. Doi, ‘Introduction to Polymer Dynamics’, Oxford Press, (1996).
- [23] M. Doi, ‘Gel Dynamics’, *J. Phys. Soc. Japan*, **78**(5), 052001 (2009).
- [24] P. J. Flory, ‘Principles of Polymer Chemistry’, Cornell University Press, Ithaca, NY, (1953).
- [25] Lin-Gibson S., Bencherif S., Cooper J.A., Wetzel S.J., Antonucci J.M., Vogel B.M., Horkay F. and Washburn N. R., ‘Synthesis and characterization of PEG dimethacrylates and their hydrogels’, *Biomacromolecules* **5**, 1280-1287 (2004).
- [26] Barbosa, I. Garcia S., Barbier-Chassefiere V., Caruelle J.P., Martelly I. and Papy-Garcia D., ‘Improved and simple micro assay for sulfated glycosaminoglycans quantification in biological extracts and its use in skin muscle tissue studies’, *Glycobiology* **13**, 647-653 (2003).
- [27] R. A. Milch, ‘Hydrated density of chondroitin sulfate preparations’, *Cell. Mol. Life Sci.*, **21**(10) 578-579 (1965).
- [28] Bryant S. J., Arthur J. A. and Anseth K. S., ‘Incorporation of tissue-specific molecule alters chondrocyte metabolism and gene expression in photocrosslinked hydrogels’, *Acta Biomaterialia*, **1** 243-252 (2005).
- [29] A. F. M. Barton, ‘Handbook of polymer-liquid interaction parameters and solubility parameters’, *CRC press* (1990).
- [30] Coleman T.F. and Li Y., ‘On the convergence of reflective newton methods for large-scale nonlinear minimization subject to bounds’, *Math. Program* **67**(2), 189-224 (1994).